

**A MODEL OF A HYBRID POWER PLANT WITH WIND TURBINES AND COMPRESSED AIR ENERGY STORAGE**

**I.Arsie**

**V.Marano**

**G.Nappi**

**G.Rizzo**

DIMEC, University of Salerno, Fisciano (SA) - Italy – Email: grizzo@unisa.it

**ABSTRACT**

After a general overview of Hybrid Power Plants (HPP) and Compressed Air Energy Storage (CAES), the authors present a thermo-economic model for the simulation and optimization of a HPP consisting of a wind turbine coupled with CAES. In the proposed scheme, during periods of excess power production, atmospheric air is compressed in a multi-stage compressor and cooled; when there is power demand, the compressed air is heated in multiple expansion stages using the stored heat and conventional thermal sources.

Such plants can offer significant benefits in terms of flexibility in matching a fluctuating power demand, particularly when renewable sources, characterized by high and often unpredictable variability, are utilized. The possible advantages in terms of energy and cost savings with respect to other solutions must be carefully assessed, critically depending on performance and efficiencies of each sub-system, most of them operating in transient and off-design conditions.

To this purpose, a thermodynamic model composed of several sub-systems describing wind turbine, multi-stage compressor, intercooler, aftercooler, heat recovery system, compressed air storage and turbine has been developed in Matlab/Simulink® environment. In the paper, several scenarios are compared by simulation and optimization analysis and a parametric study of the plant performance with respect to the main design variables is presented.

**INTRODUCTION**

As it is known, some of the major limitations of renewable energy sources are represented by their low power density and intermittent nature, largely depending upon local site and unpredictable weather conditions [1]. These problems concur to increase the unit costs of the energy obtained by renewable sources, so limiting their diffusion and the benefits due to the reduced exploitation of fossile resources [2].

A possible solution to this problem may be the simultaneous utilization of two or more energy resources within a Hybrid Power Plant (HPP). In this case, the recourse to multiple energy sources, both renewable or traditional, can effectively mitigate the effects of their variability. The applications of HPP cited in literature, range from use of Photo-Voltaic (PV) and Wind Systems [1]-[4], to Wind-Diesel Systems [5], [6], to Systems combining Wind, Solar and Diesel [7], [8], [9].

The recourse to appropriate energy storage systems may be also necessary both to compensate the residual variability of the input energy from renewable sources, and, moreover, to match a fluctuating power demand [10]. The most widely used energy storage systems are batteries, Hydraulic Pumped Storage (HPS) and Compressed Air Energy Storage (CAES), while energy storage systems under development include regenerative fuel cells, superconductive magnets and flywheels.

**NOMENCLATURE**

<i>Greek Symbol</i>	<i>Description</i>	<i>Unit</i>
$\beta$	Pressure ratio	/
$\eta$	Efficiency	/
$\rho$	Incoming wind density	kg/m <sup>3</sup>

<i>Latin Symbol</i>	<i>Description</i>	<i>Unit</i>
A	Cross-sectional area of stream	m <sup>2</sup>
c <sub>p</sub>	Specific heat at constant pressure	kJ/kgK
c <sub>v</sub>	Specific heat at constant volume	kJ/kgK
DC	Daily electric energy consumption	kWh
E	Electric energy	kJ
E <sub>qh</sub>	Equivalent hours	h
h	Enthalpy	kJ/kgK
H <sub>i</sub>	Fuel heating value	kJ/kg

IC	Instantaneous consumption	kWh
k	Specific heat ratio ( $c_p/c_v$ )	/
m	Mass	kg/s
MC	Monthly electric energy consumption	kWh
ML	Maximum electric load	KW
n	Rotating speed	rpm
p	Pressure	bar
P	Mechanical power	kW
Q	Heat	kW
R	Gas constant	kJ/kgK
T	Temperature	K
U	Internal energy	kJ
v	Wind speed	m/s
V	Volume	m <sup>3</sup>

*Subscripts*                      *Description*

0	Design value
AC	Aftercooler
C	Compressor
f	Fuel
h <sub>2</sub> o	Water
IC	Intercooler
in	Inlet
out	Outlet
R1	Regenerator 1
R2	Regenerator 2
red	Reduced parameter
T	Turbine
WT	Wind turbine

*Superscripts*                      *Description*

—	Divided by design value
•	Instantaneous value

**CAES**

In CAES, energy is stored in the form of compressed air in a reservoir, usually an underground cavern (salt dome, aquifer and rock caverns) [1], [11], [12], [13].

In these plants, air is compressed and stored during off-peak periods, while the thermal energy extracted by the compressor coolers is stored as heat; the accumulated energy is then used on demand during peak periods to generate power with a turbo-generator system: in this case, all the power of the turbine can be used to generate electricity, while in conventional gas turbine plants a significant fraction of turbine power is utilized by the compressor. Two different approaches to cavern design are adopted: constant volume (un-compensated), where pressure can change during the process, and constant pressure (compensated), where water from a surface reservoir displaces the compressed air to maintain a constant pressure in the reservoir.

Unlike gas turbines, also utilized for peak lopping applications, the systems based on energy storage allow to accumulate the excess energy produced during periods of low load demand, returning it during peak load periods. However, HPS has high capital cost and requires a difference in geodetic height, a condition that could be not satisfied in flat regions [11].

For these reasons, an increasing attention has being paid in recent times to CAES, that could represent a feasible solution, particularly in flat areas. Recent studies using simulation models have shown the advantages of CAES respect to HPS in terms of Energy Ratio and primary energy efficiency [11], [14]. A further advantage of this technology is represented by the fast start-up. A CAES plant can provide a start-up time of about 9 minutes for an emergency start, and about 12 minutes under normal conditions, while conventional gas turbine peaking plants typically require 20 to 30 minutes for a normal start-up.

The first commercial scale CAES plant in the world is the 290MW Huntorf, Germany, operated by Nordwest Deutsche Kraftwerke (NDK) since 1978. The Huntorf plant, with a salt cavern, runs on a daily cycle in which it charges the air storage for 8 hours and provides generation for 2 hours. The plant has reported high availability of 86% and a starting reliability of 98%. The Alabama Electric Co-operative Inc. in McIntosh (Alabama) built the second commercial scale CAES plant [15], with a cavern capacity of around 1.8 million cubic metres and 110 MW of power generation. This plant exhibits a 74.7% “thermal efficiency” with a charging ratio of 1.3. Other plants are active or in construction in Japan (35MW) and Israel (100MW).

Some aspects related to the combination of CAES with a conventional Gas Turbine Power Plant, with respect to “classical” CAES concept, requiring ad hoc design for expander train and combustor, have also been recently discussed [16], [17], [18].

**INTEGRATION OF CAES WITH WIND**

In spite of CAES remarkable capabilities in compensating power fluctuations not only on output side (power demand), but also on input side, little attention has been paid in literature to use of CAES with renewable energy sources, like wind and solar, within a Hybrid Power Plant (HPP) concept [19]. The present paper is therefore focused on the combination of CAES with a wind turbine (or a wind farm). The proposed plant could also be further integrated with solar energy, to pre-heat the air extracted from the reservoir by means of thermal solar panels, or to integrate the electrical power via Photo-Voltaic systems. Extensions to these cases will be analyzed in next future.

Of course, the main drawback of a solution combining two or more energy sources with an appropriate storage system is the significant increase of investment costs, due to larger plant complexity. For CAES, a significant contribution to the cost is the construction of the underground cavern. Therefore, careful plant design and investment analysis are required in order to assess their convenience with respect both to conventional plants and to plants based on a single renewable source. On the other hand, the presence of two or more energy sources, the intrinsic variability and uncertainty related to renewable energy availability, the need to adopt suitable strategies to manage the energy storage system in presence of an unknown future energy demand depict a very complex scenario and make the analysis of these plants a very difficult task.

To face this problem, complex model based methodologies are needed in order to determine the best plant structure and its optimal operation and scheduling, as a function of plant location and power demand.

In the following chapters, a model of a Hybrid Power Plant combining wind energy and thermal energy derived by fossil fuels with a CAES is presented.

**POWER PLANT SCHEME AND MODEL**

The scheme of the proposed plant is presented in Fig. 1. It consists of these basic components:

- Wind Turbine (WT) with electric generator;
- Compressor train (two stages compressor C1-C2, inter-cooler IC and after-cooler AC);
- Motor/Generator M/G;
- Clutch F;
- Compressed Air Storage (cavern) S;
- Valve V, to control the air flow from and to the cavern.
- Turbine expander train (including two stages expanders T1-T2 and combustors CC1-CC2);
- Regenerator R;
- Thermal Reservoir for Heat Recovery HR;
- Connection to grid power GP, for managing integrations and/or surplus.
- Electric User U.

Electricity from WT and/or from GP powers an electric motor M, which drives a two-stages air compressor C1-C2.

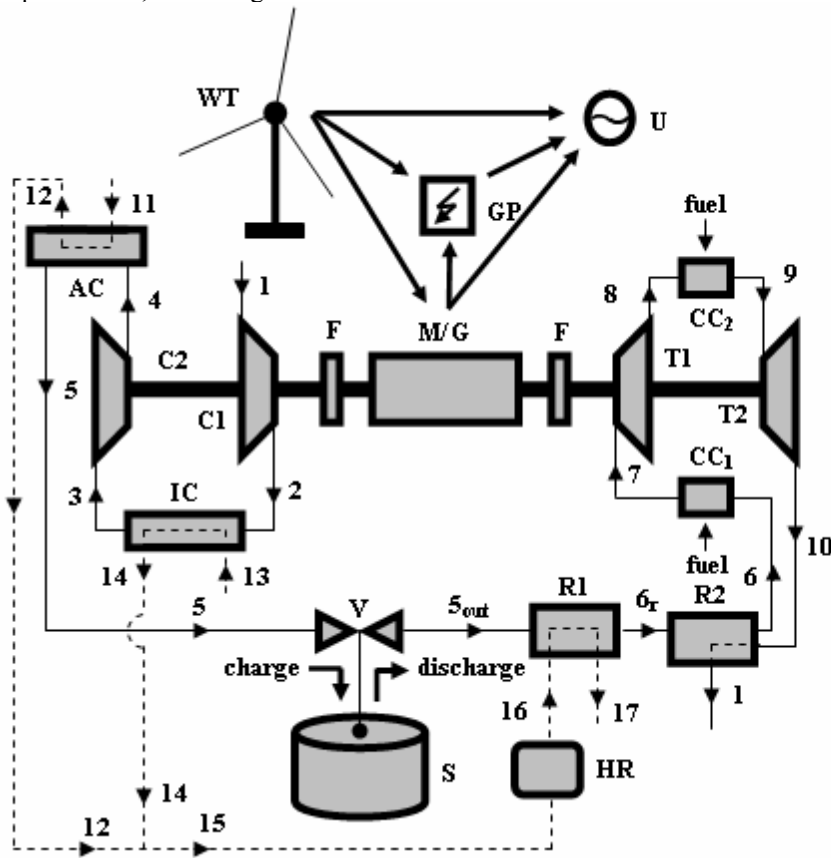
The heat generated by the compression process is extracted by inter-stage cooling IC and after cooling AC and stored in a recuperator HR, consisting in a hot water reservoir. Most of the

energy from wind and/or grid is therefore stored as pressure potential energy of the compressed air in the cavern S. When air is extracted from S, it is preheated in the recuperator R1, utilizing the heat extracted from compression process, and then in a second recuperator R2, utilizing the heat at the discharge of turbine T2. The air is then mixed with fuel, burned in the combustor CC1 and expanded in a first turbine T1. A second combustor CC2 is then used, before the second expansion in T2. The residual heat of the discharge gas is the used to pre-heat the air before the combustor in the recuperator R.

Different operation modes can be considered in this plant. Energy from WT can be provided to the motor M, to the grid GP or directly to the user U. Grid power (GP) can be supplied to the user U, while the electricity generated from G can be provided to grid GP or to the user U. Consequently, the valve V manages the corresponding charge or discharge processes.

As shown in the next chapters, the optimal plant management strategies can be computed by minimizing the operational costs over a prescribed time horizon (typically, a day), with proper constraints over the energy content of the reservoirs.

The most important assumptions and relationships adopted to model the power plant components are presented in the following.



AC	Aftercooler
C	Compressor
CAES	Compressed Air Energy Storage
CC	Combustion Chamber
F	Clutch
GP	Grid Power
HR	Heat Recovery
IC	Intercooler
M/G	Motor/Generator
R1	Regenerator 1
R2	Regenerator 2
S	Air Storage
T	Turbine
U	User
V	Valve
WT	Wind Turbine

Fig. 1 – Power Plant Scheme

## WIND TURBINE

The power from wind turbine can be determined by the following relationship:

$$(1) \quad P_{WT} = \frac{1}{2} \rho A v^3 \eta_{WT}$$

where the efficiency  $\eta$  can be expressed as function of wind speed  $v$ . The main data of the wind turbine (AWT-26 [20]) are reported in Tab. I. The efficiency curve, represented in Fig. 2 has been derived from a turbine with similar power and wind density.

The computation presented in the following have been performed with respect to the daily wind speed profile presented in Fig. 3. The corresponding profile of the wind turbine efficiency is shown in Fig. 4. Finally, the comparison between the net wind turbine power and the required power is presented in Fig. 9.

As power demand, a typical profile during a working day at the Campus of the University of Salerno, Italy, has been selected. Average power level (about 1 MW) is in this case significantly lower with respect to the applications of CAES reported in previous chapter.

On the other hand, the proposed model and the methodology are very general and scalable, and the conclusions not affected by the selected power level.

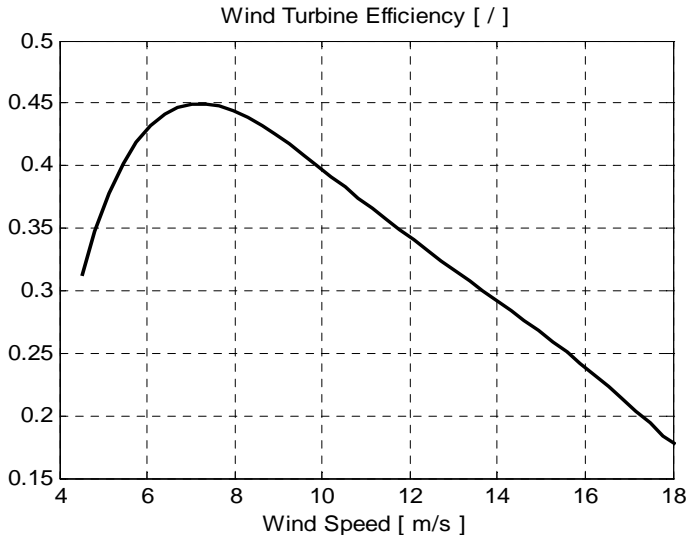


Fig. 2 – Wind turbine efficiency vs. wind speed

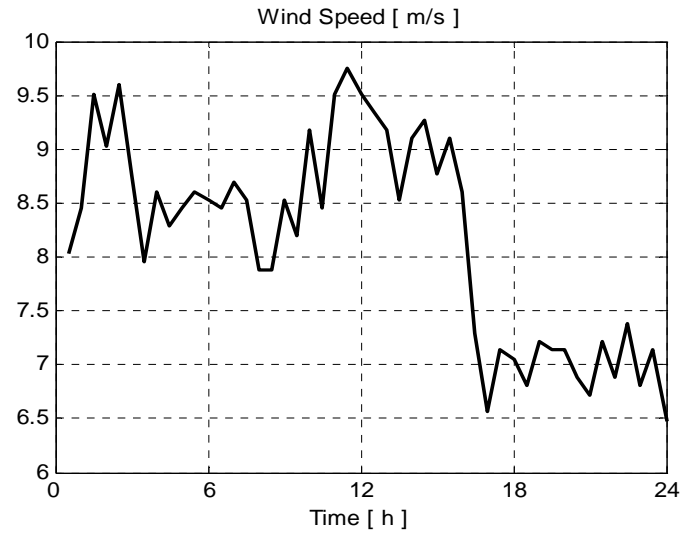


Fig. 3 – Time history of the wind speed along the day

Wind turbine	
Wind turbine radius	45 [ m ]
Wind tower height	60 [ m ]
Cross-sectional area of stream	11304 [ m <sup>2</sup> ]
Rated Power	1500 [ kW ]
CAES plant	
Compressed air reservoir volume	2000 [ m <sup>3</sup> ]
Thermal reservoir height	7 [ m ]
Thermal reservoir radius	1.5 [ m ]
Thermal reservoir volume	49.455 [ m <sup>3</sup> ]

Tab. I – Plant Data

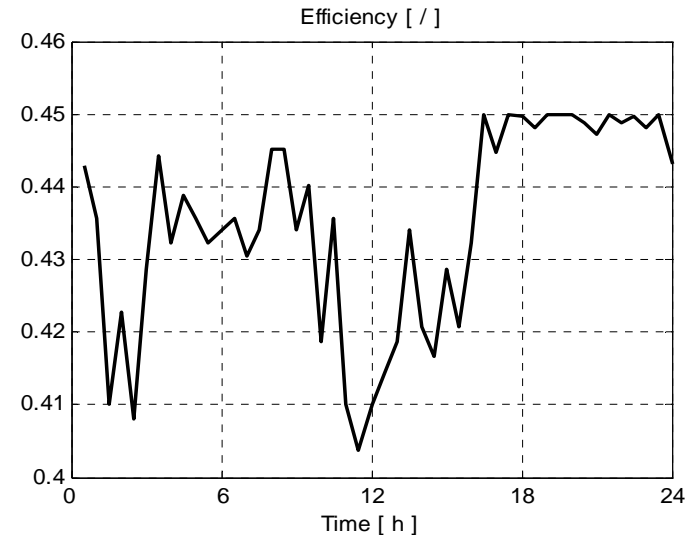


Fig. 4 – Time history of wind turbine efficiency

## COMPRESSOR

The use of a two stages reciprocating compressor C1-C2 with the same compression ratio, with inter-cooler IC and after-cooler AC, has been assumed. The power for each

compression stage can be computed by well known relationships:

$$(2) \quad P_C = \frac{1}{\eta_C} \dot{m} c_p T_{in,C} \left( \beta^{\frac{k-1}{k}} - 1 \right)$$

In order to take into account the effects of part-load operation, the ratio between actual and maximum adiabatic efficiency has been expressed as function of the ratio between actual and maximum power (Fig. 5), starting from literature data for reciprocating compressors [21].

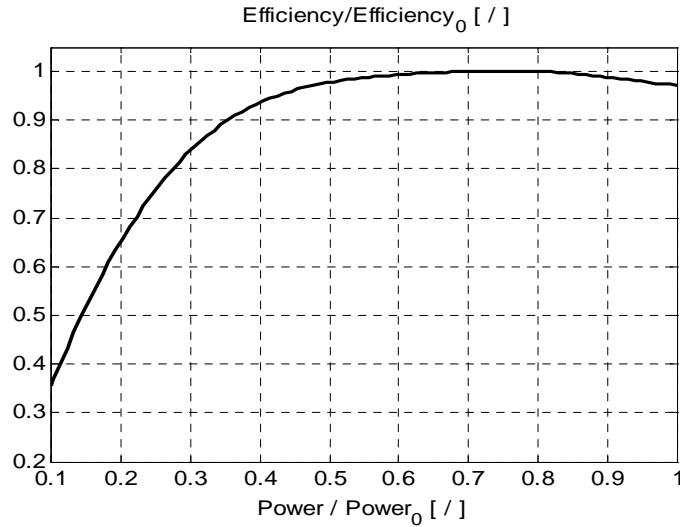


Fig. 5 – Relative variation of compressor efficiency vs. power.

### TURBINE MODEL

The operation of each turbine stage is described by means of the reduced parameters:

$$(3) \quad \dot{m}_{red,T} = \frac{\dot{m}_T}{P_{in,T}} \sqrt{T_{in,T}}$$

$$(4) \quad n_{red,T} = \frac{n_T}{\sqrt{T_{in,T}}}$$

An improved Flügel formula is used to approximately describe the mass flow characteristics of the turbine [22]:

$$(5) \quad \bar{m}_T = \alpha \sqrt{\frac{T_{in,T}}{T_{in,T,0}}} \sqrt{\frac{(\beta^2 - 1)}{(\beta_0^2 - 1)}}$$

where the factor  $\alpha$  accounts for the influence of rotating speed:

$$(6) \quad \alpha = \sqrt{1.4 - 0.4 \left( \frac{n_T}{n_{T,0}} \right)}$$

Turbine adiabatic efficiency is calculated as

$$(7) \quad \bar{\eta}_T = \left[ 1 - t(1 - \bar{\eta}_{red,T})^2 \right] \left( \frac{\bar{\eta}_{red,T}}{\bar{m}_{red,T}} \right) \left( 2 - \frac{\bar{\eta}_{red,T}}{\bar{m}_{red,T}} \right)$$

where it is assumed  $t = 0.3$ .

The above diagrams describe the variations of turbine adiabatic efficiency (Fig. 6) and mass flow rate (Fig. 7) with power and expansion ratio. In the present application, the rotational speed has been assumed constant (3000 rpm).

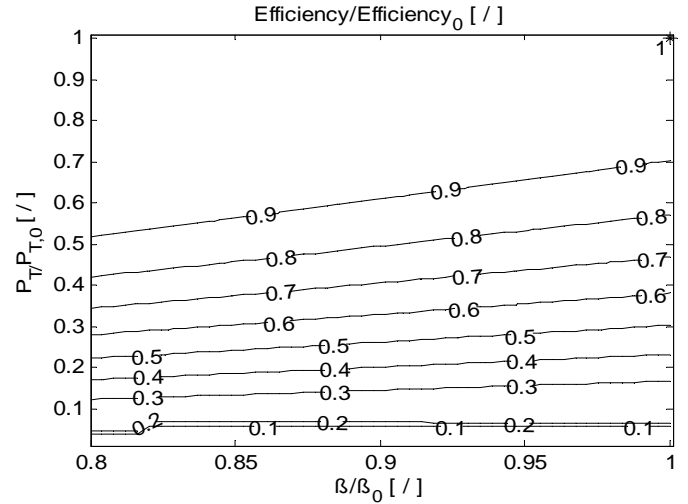


Fig. 6 - Effects of expansion ratio and power on turbine adiabatic efficiency

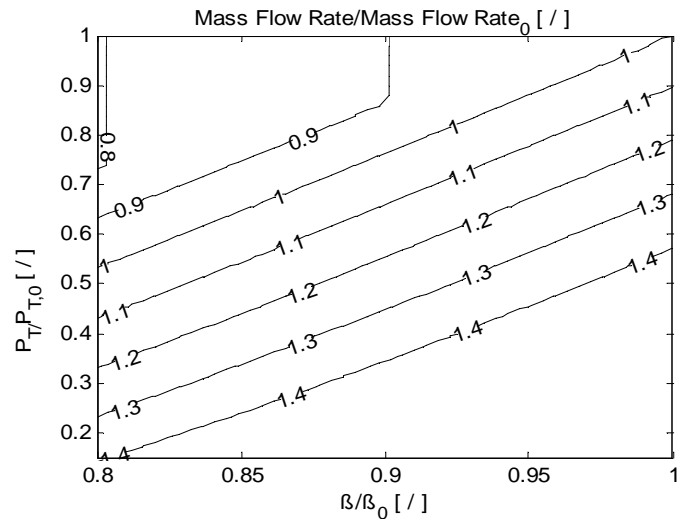


Fig. 7 – Effects of expansion ratio and power on mass flow rate

### COMPRESSED AIR RESERVOIR

For the air storage S, a conventional “un-compensated” constant volume cavern has been assumed, with a volume of 2000 m<sup>3</sup>. Air pressure ( $P$ ) and temperature ( $T$ ) during charging and discharging processes can be computed by mass and

energy balance in unsteady regime and from gas state equation in differential form, through the above equations.

Due to the large capacity of the cavern and the relatively short residence time, heat losses have not been considered.

$$(8) \quad \frac{dU}{dt} = \dot{m}_{in} \cdot h_5 - \dot{m}_{out} \cdot h_{5,out}$$

$$(9) \quad \frac{d\left(\frac{p}{T}\right)}{dt} = \frac{d}{dt}(m \cdot R/V) = (R/V) \cdot \frac{dm}{dt} = \dot{m} \cdot \frac{R}{V}$$

$$(10) \quad \frac{dp}{dt} = \frac{K \cdot R}{V} \cdot (\dot{m}_{in} \cdot T_5 - \dot{m}_{out} \cdot T)$$

$$(11) \quad \frac{dT}{dt} = \frac{K \cdot \dot{m}_{in} \cdot T_5}{m} + \frac{[\dot{m}_{out} \cdot (1-K) - \dot{m}_{in}]}{m} \cdot T$$

### THERMAL RESERVOIR

Thermal energy extracted from IC and AC is stored in a variable mass hot water reservoir of 50 m<sup>3</sup>, and used in the regenerator R1 to pre-heat the air. Mass and energy balance can be performed to compute mass and temperature in the reservoir, also considering thermal losses.

$$(12) \quad \frac{dU}{dt} = \dot{m}_{IC} \cdot T_{IC} \cdot c_{h_2o} - \dot{m}_{AC} \cdot T_{AC} \cdot c_{h_2o} - \dot{m}_{R1} \cdot T_{R1} \cdot c_{h_2o} - \dot{Q}_{lost}$$

### THE ECONOMIC MODEL

The economic model evaluates the daily operational costs due to the electrical energy and the methane purchased from the respective providers (in Italy) [23]; the model also considers the possible revenues due to the sale of electric energy surplus.

The costs due to the methane delivered to the combustion chambers is composed of a fixed term and a variable term, both depending on the annual consumption according with the fees reported in Tab. II.

Annual Consumption		Unitary Cost	Fixed Cost
From [m <sup>3</sup> /year]	To [m <sup>3</sup> /year]	€m <sup>3</sup>	€/year
1	250	0.298	15
251	1001	0.308	60
1002	2501	0.291	65
2502	25013	0.327	20
25014	200100	0.307	15
200101	Inf	0.267	0,05 · Daily Consumption [m <sup>3</sup> ]

Tab. II – Fees for the methane supply

The electrical energy cost is estimated by the following relationship:

$$(13) \quad EC = \frac{C1+C2+C4}{30} + C3$$

where **C1**, **C2** and **C4** are the monthly costs in [€/month] imposed by the provider and expressed as

$$(14) \quad C1 = 1.80 \cdot ML$$

$$(15) \quad C2 = 29.2309$$

$$(16) \quad C4 = A1 \cdot MC$$

where A1 is 0.0108 when MC is lower than 8·10<sup>6</sup> kWh and is 0.001 otherwise.

The term **C3** depends on the actual electrical energy cost, which is variable along the day according with the graph in Fig. 8. The three cases mentioned in the figure depend on the ratio between monthly energy consumption and maximum requested power expressed by the parameter E<sub>qh</sub> as:

$$(17) \quad E_{qh} = \frac{MC}{ML}$$

The daily electrical energy cost C3 in [€/day] is then estimated by the following relation:

$$(18) \quad C3 = \int_0^{86400} (EEC(t) \cdot IC(t)) dt$$

The total daily cost of the electrical energy is finally computed as:

$$(19) \quad TC = 1.2 \cdot (EC + Tax) - ER$$

where Tax and electrical energy revenue (ER) are given by the following relationships:

$$(20) \quad Tax = 0.0124 \cdot DC$$

$$(21) \quad ER = 0.052 \cdot Energy_{SOLD}$$

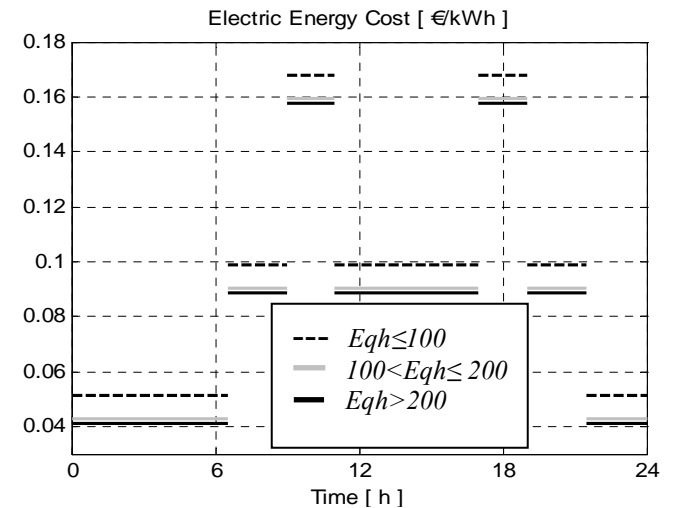


Fig. 8 - Electric Energy Component Cost EEC

## PLANT EFFICIENCY AND ENVIRONMENTAL IMPACT

Apart from the economic analysis, a global efficiency has been introduced to compare the proposed test cases from an energetic point of view. In case of HPP (test case 1), the global efficiency has been defined as ratio between the electrical energy provided to user and grid by wind turbine and CAES during the assumed time horizon (24 hours), and the corresponding primary (source) energy:

$$(22) \quad \eta = \frac{E_{out}}{\frac{E_{WT}}{\eta_{WT}} + m_f H_i}$$

where the denominator accounts for the fuel provided to the CAES and the primary wind energy.

For the test case 2, the global efficiency is given as the ratio between the electrical energy provided by the wind turbine and the primary wind energy, thus corresponding to the mean value of the wind turbine efficiency.

In case of CAES plant coupled with grid (test cases 3A and B), the global efficiency is given as the ratio between the electrical energy provided by the CAES to user and grid and the primary energy provided to the CAES:

$$(23) \quad \eta = \frac{E_{out}}{\frac{E_{GP}}{\eta_{GP}} + m_f H_i}$$

where the denominator accounts for the fuel and the equivalent primary energy of the electrical energy supplied by the grid. This latter is computed according with the standard efficiency of the national grid power for Italy, which has also been assumed as global efficiency for the last test case (test case 4).

It is worth to note that in case of HPP with CAES, the primary energy considered for evaluating the global efficiency is obtained summing up the contributions due to both renewable and non renewable energy sources.

In order to evidence the different environmental impact of these solutions, CO<sub>2</sub> emissions have been estimated for the examined test cases (Tab. III), separately considering the emissions produced on the plant and those corresponding to the purchased grid power. In both cases, it is assumed that CO<sub>2</sub> is produced burning methane. Of course, this simplifying assumption does not take into account that grid power is produced by a mix of power plants, with different environmental impact [24]. In order to compare homogeneously the different solutions, the energy globally produced by each case has been also evidenced, summing up the energy to the user and the one sold to the grid. The last column reports therefore the specific CO<sub>2</sub> emissions.

Of course, a careful study of the environmental impact of the “emission-free” power plants could not aside from an analysis of Life Cycle Assessment [25], considering all the processes involved in the construction, operation and demolition of the power plants.

## OPTIMAL PLANT MANAGEMENT AND DESIGN

The study of a plant including an energy storage has an intrinsic grade of complexity, due to the fact that it must be necessarily performed in transient conditions, and considering the off-design operation of the various components. Due to the typical use of CAES, the computation has been carried out with reference to daily cyclic generation. In order to compare in a homogeneous way different plant schemes and various management strategies in terms of operational costs and energy consumption, it is also necessary that the energy content of the reservoirs S and HR (Fig. 1) at the end of the time horizon does not vary with respect to the initial value.

The proposed model allows to perform daily cycle computations with optimization of both design and management variables via non-linear programming techniques [26], [27], [28] assuming the daily operational cost as objective function to be minimized. As described in the previous section, the daily operational cost accounts for the purchase of electrical energy and methane and for the sale of the electrical energy surplus.

Classical mathematical programming techniques, implemented in Matlab/Simulink® environment, have been used. The formulation of the constrained minimization problem is:

$$(24) \quad \min_x f(x) \quad [\text{non-linear objective function}]$$

$$(25) \quad C(x) \leq 0 \quad [\text{non-linear inequality constraints}]$$

$$(26) \quad L_b \leq x \leq U_b \quad [\text{lower and upper bounds}]$$

where  $x$  is the vector of the design (and control) variables.

The optimum problem (eqs. 24-26) is solved by a second-order Sequential Quadrating Programming approach. The recursive Hessian matrix estimate is performed by the BFGS method. The inequality constraints account for *i*) the difference between initial and final temperature and pressure in the cavern (S), *ii*) the pressure in the cavern between 40 and 80 bar, *iii*) the water temperature in the recuperator (HR) greater than 273.15 K, *iv*) the difference between initial and final values for mass and temperature in the recuperator (HR).

The optimization analysis is carried out in case of two different plants, with or without the wind turbine. Moreover, in the former case, when the wind turbine is present, the operation of the plant can be distinguished in two modes: *i*) energy storage mode, when the wind power exceeds the load power and *ii*) generation mode otherwise. In case of energy storage, the vector of design variables  $x$  is given as the fraction of the extra power delivered by the wind turbine which is supplied to the electric motor (M/G) to run the compressors, computed at each time step (one hour):

$$(27) \quad x_i = \frac{P_{storage_i}}{P_{wind_i} - P_{load_i}}$$

The design variable  $x_i$  is constrained between 0 and 1; thus, the load power requested by the user is completely satisfied by the wind turbine; moreover when  $x_i < 1$ , the power surplus  $(1 - x_i) * (P_{wind_i} - P_{load_i})$  is sold to the grid.

In case of generation, when the load power exceeds the wind power, the design variable is computed at each time step as the ratio between the power delivered by the turbines and the extra power needed to meet the user requirements:

$$(28) \quad x_i = \frac{P_{generation_i}}{P_{load_i} - P_{wind_i}}$$

The design variable  $x_i$  is still constrained between 0 and 1; thus the power delivered by the wind turbine is exclusively used to satisfy the load power; moreover when  $x_i < 1$ , the extra power  $(1 - x_i) * (P_{load_i} - P_{wind_i})$  is purchased by the grid.

In case of a standard CAES plant without wind turbine, the plant design is simpler due to the reduced number of possible operational modes; in such case, the design variable  $x_i$  is defined as the power purchased by the grid, both for powering the compressor and for satisfying the load requirements.

In all cases the design variables vector  $x$  is augmented including the design power of compressors and turbines: the optimization process is therefore carried out with respect to 26 variables.

Sensitivity analysis of the optimal solutions can be also performed, in order to check the feasibility of the proposed solutions. The model can also be used in simulation mode and

for parametric analysis with respect to design variables: some examples are shown in next chapter.

## RESULTS

The optimization analysis has been carried out considering different test cases, as summarized in Tab. III. The first case refers to the power plant scheme shown in Fig. 1, composed by wind turbine and CAES, including their respective interactions with grid and user. The following cases 2 and 3 are derived from the first, neglecting the CAES or the wind turbine respectively. The last CAES considers the conventional purchase of electrical energy from the grid.

All the test cases have been analyzed considering the time history of electrical load required by the user shown in Fig. 9. The figure also depicts the electrical power provided by the wind turbine, evidencing that it exceeds the load power in the early morning, until approx. 9.00 a.m., and at night, after approx. 8.00 p.m.; in the meantime, from 9.00 a.m. to 8.00 p.m., the load power exceeds the power delivered by the wind turbine, which need to be integrated in some way. The optimization analysis has then been focused on the management of the energy flows between wind turbine, CAES and grid power in order to accomplish the user requirements and minimize the operational cost of the plant along the assumed time horizon (i.e. 24 hours).

Test Cases		Daily Cost [€/day]	Efficiency [%]	CO <sub>2</sub> From plant [kg/day]	CO <sub>2</sub> From GP [kg/day]	CO <sub>2</sub> Total [kg/day]	Produced Energy [kWh/day]	Spec.CO <sub>2</sub> emissions [kg/kWh]
1. Wind + CAES + Grid Power		284	38.7	645	577	1222	22548	0.054
2. Wind + Grid Power		524	43.5	0	2273	2273	26269	0.087
3. CAES + Grid Power	A. Grid power to CAES can only be purchased in the early morning and at night	2372	36.5	2789	8388	11186	20798	0.538
	B. Grid power to CAES can be purchased at any time during the day	2224	39.3	2879	7990	10869	21613	0.503
4. Only Grid Power		2968	37.5	0	10897	10897	20684	0.527

Tab. III – Test Cases and Global Results

The optimization results achieved for the first test case are summarized in Fig. 10. The figure shows the time history of the global electrical power provided by the wind turbine, the electrical power requested by the user and the output electrical power provided to both user and grid. The behavior of the three mentioned power profiles can be better clarified by analyzing their values at three time instants, corresponding to 6.00, 18.00 and 24.00. In the former case, the wind power exceeds the load power; thus, a fraction of it is used to meet the user requirement (segment C-D), while the extra power is partially provided to the compressors (segment A-B) and partially sold to the grid (segment B-C). On the other hand, at the time 18.00, the electrical load exceeds the wind power, which is not sufficient to meet the user requirement; therefore, this latter is accomplished partially by the wind turbine (segment G-H), partially by the CAES (segment F-G) and partially by purchasing the energy from the grid (segment E-

F). At the time 24.00 the wind power is still greater than the electrical load, but unlike the previous case at 6.00, the extra power is sold to the grid instead of being stored in the CAES by driving the compressors. This behavior is due to the imposed constraints on the cyclic fluctuations of temperature and pressure in the air reservoir over the daily operation. The various operational modes depicted in the figure evidence the complexity of the optimization analysis which involves a considerable number of variables (up to 26). The operational modes of the CAES plant can also be detected from Fig. 11, which shows the inlet and outlet air mass flow in the air reservoir. In the early stages, when the wind power exceeds the electrical load, the extra power drives the compressors, thus enhancing the the air storage into the reservoir. Then, as the electrical load increases, the CAES provides the electrical power needed to accomplish the user requirements by discharging the air reservoir. In the latter part of the time

history, both inlet and outlet mass flow are zeroed, since the extra power provided by the wind turbine is sold to the grid. Fig. 12 shows the time history of compressor and turbine efficiency, evidencing that for most of the time, their working conditions are very close to the nominal ones. It's worth to note that the turbine and compressor efficiencies are zeroed during storage and generation phase, respectively. The satisfactory efficiency achieved along the whole working cycle is also confirmed by the histogram shown in Fig. 13, which evidences that compressor and turbine work at maximum efficiency for approx. 80 % and 55 % of the time, respectively. The lack in turbine performance can be explained through Fig. 14, which exhibits some fluctuations of the inlet turbine temperature. Fig. 15 and Fig. 16 show the time histories of pressure and temperature in the air reservoir and water mass and temperature in the thermal reservoir, respectively. The figures exhibit the initial increase due to the air storage in the early stages followed by the decrease when the CAES works in generation mode. The figures also evidence that the constraints imposed on the cyclic behavior along the daily operation are satisfied for all the variables, with minor tolerance.

The optimization results achieved in the test cases 3A and 3B are summarized in Fig. 17 and Fig. 18 which show the time history of the electrical power requested by the user, the grid power provided to the CAES and the output power provided to user and grid. Fig. 17 refers to the case 3A, where the grid power can be provided to the CAES only in the time window from 21.30 to 6.30 when its cost is more convenient. The figure shows that a large power is purchased from the provider to the CAES in the early morning in order to store a satisfactory amount of compressed air. During the day time (i.e. 18.00), the air storage is disabled and the electrical load is partially provided by the CAES (segment B-C), partially by the grid (segment A-B).

In the test case 3B (see Fig. 18), the grid power can be provided to the CAES at any time; it is still noticeable a large storage of air in the early morning, when the electrical energy provided by the grid is cheaper; on the other hand, at midday (i.e. 12.00), the CAES works in generation mode, providing all the electrical load required by the user (segment B-D) and selling the extra power to the grid (segment A-B). At the same time a small amount of power is purchased from the grid (segment C-D) in order to store compressed air and keep an adequate pressure in the air reservoir. At 18.00 the CAES provides most of the electrical power requested by the user (segment F-H), while the grid provides the power for the air storage (segment G-H) and the electrical load left (segment E-F).

Fig. 19 and Fig. 20 show the time histories of pressure and temperature in the air reservoir for the two test cases 3A and 3B. In both cases temperature and pressure exhibit a general increase in the early stages when most of the air storage takes place and a reduction in the latter part of the day when the CAES provides power to the user. Nevertheless in the case 3B, a significant increase of pressure and temperature occurs even at midday, when storage and generation modes are operated simultaneously. The figures also evidence that the constraints on temperature and pressure fluctuations over the whole day are satisfied in both cases, with the final values approaching the initial ones with a satisfactory approximation.

The global results of the optimization analyses performed in the proposed test cases are summarized in Tab. III, by the daily operational cost, the global efficiency and the CO<sub>2</sub> emissions. The former is evaluated according with Tab. II and eq. (19) and evidences that the best results are achieved in case of hybrid power plant with both wind turbine and CAES. This configuration allows to manage the energy flows coming from renewable and conventional sources in the most convenient way, by storing the extra power provided by the wind turbine in the CAES and purchasing/selling electrical power from/to the grid according with the current cost.

In case of conventional wind farm with the wind turbine directly coupled to the grid (test case 2), the daily operational cost is significantly higher, due to the missing chance to store the power surplus of the wind turbine when the electrical load is lower. The operational costs dramatically increase when conventional energy sources are used without any recourse to renewable energy (test cases 3A, 3B and 4). In the former two cases the CAES plant is directly coupled with the grid and a slight decrease of the operational cost is detected for the case B, where the grid power can be provided to the CAES at any time of the day, with a better energy flow management. The last test case 4 refers to the conventional exclusive recourse to the grid power, which obviously results in the most expensive configuration.

The results in Tab. III evidence that the most convenient energy conversion from primary source to final user is achieved by conventional wind plants (43.5%), while the standard global efficiency assumed for the grid power is 37.5%. Assuming these two efficiencies as reference for conventional plants, the HPP with CAES and wind turbine reaches a satisfactory efficiency of 38.7%, lower than the wind turbine, due to the energy losses associated to the air storage and generation processes, but still greater than the grid efficiency. A good global efficiency is also achieved for the CAES plant without wind turbine, especially in the case 3B (39.3%), where a better management of incoming/outcoming energy flow from/to the grid can be achieved since electrical energy can be purchased at any time of the day.

In terms of CO<sub>2</sub> specific emissions (Tab. III, last column), it can be observed that the proposed CAES/Wind/Grid solution (Case 1) allows a reduction of one order of magnitude with respect to the conventional solution (Case 4). There is also a significant reduction (38%) with respect to the recourse to wind energy and grid (Case 2). On the other hand, the use of "classical" CAES concept does not produce significant variations in terms of CO<sub>2</sub> emissions with respect to the case 4. However, it has to be remarked that this latter result is affected by the optimistic assumption about the CO<sub>2</sub> impact of grid power production.

Fig. 21 and Fig. 22 show the results of a sensitivity analysis carried out for the HPP with CAES (test case 1), in order to evaluate the effects of the design power of turbines and compressors on the daily operational cost. The analysis has been performed assuming as default the optimal design vector  $x$ , where the design power corresponds to the optimal one ( $P_0 = P_{0,opt}$ ). In Fig. 21 the daily operational cost of the plant reaches its minimum as the compressor design power approaches the optimal one, thus confirming the optimization results; on the other hand, Fig. 22 evidences that a further reduction of the daily operational cost could be achieved by

increasing the turbine design power. The results of the optimization algorithm can then be explained considering that an increase of the turbine design power would succeed in a violation of the imposed constraints on the pressure in the reservoir, thus being infeasible with the given reservoir capacity and the proposed management strategy. This behavior is shown in Fig. 23 where the initial and final values of the air reservoir pressure are plotted vs. the design power of the turbine. The figure also illustrates the acceptable range of the final pressure in order to meet the imposed constraints.

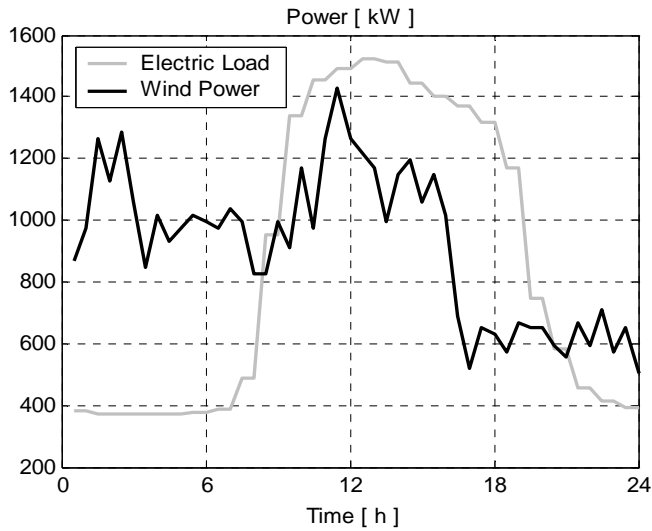


Fig. 9 – Time history of electrical load and wind power

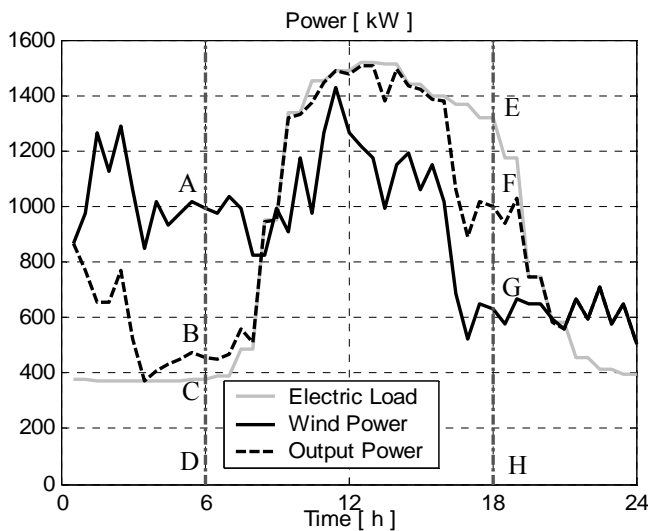


Fig. 10 – Time history of wind power, electrical load and output power (Test Case 1)

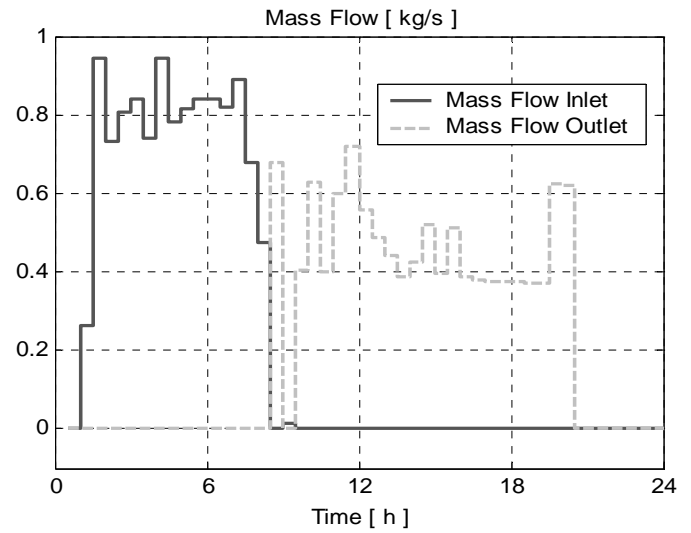


Fig. 11 – Time history of inlet and outlet air mass flow rate in the air reservoir (Test Case 1)

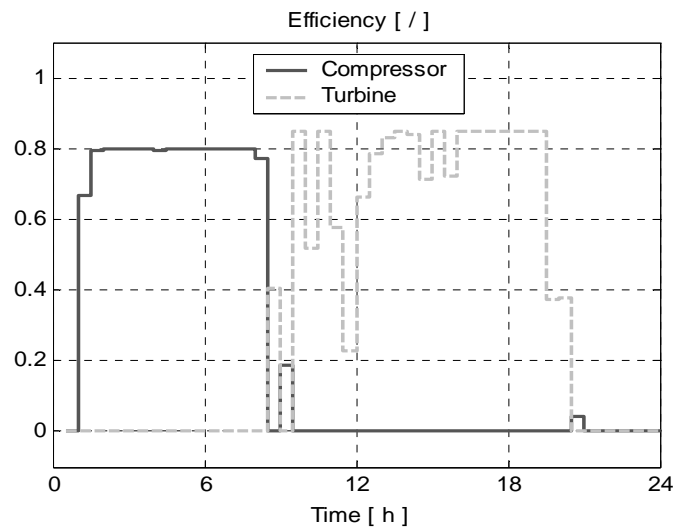


Fig. 12 – Time history of compressor and turbine efficiency (Test Case 1)

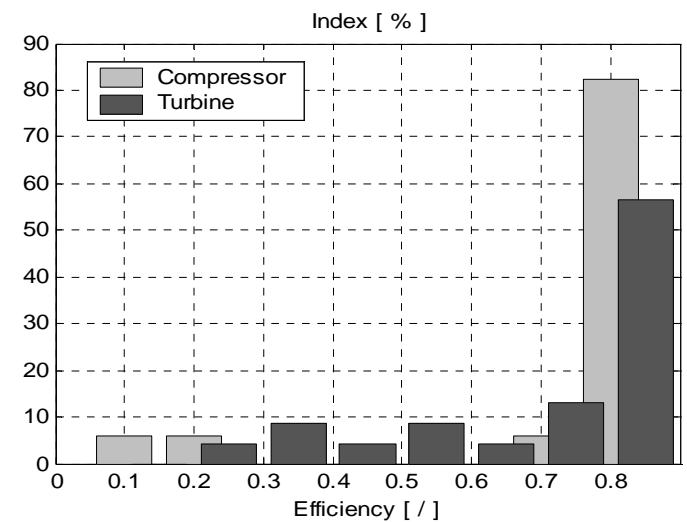
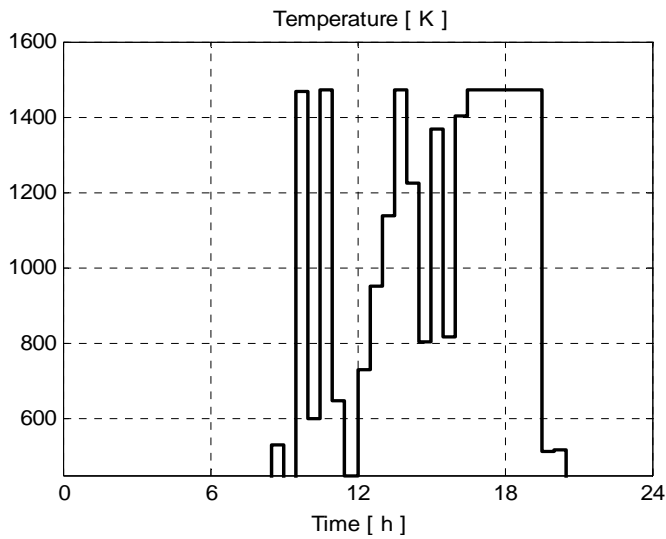
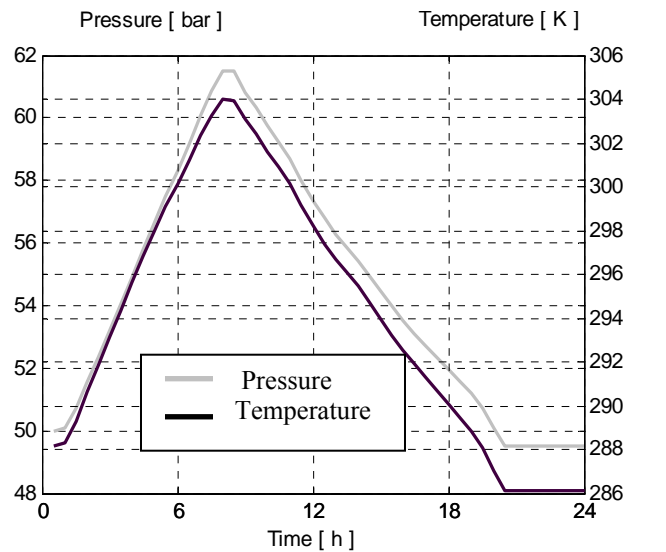


Fig. 13 – Histogram of turbine and compressor efficiency (Test Case 1)



**Fig. 14 – Time history of inlet turbine temperature (Test Case 1)**



**Fig. 15 – Time history of pressure and temperature in the air reservoir (Test Case 1)**

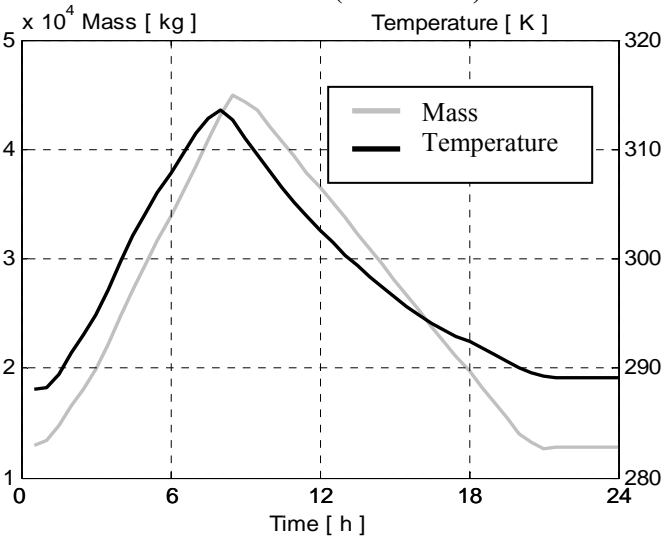


**Fig. 16 – Time history of water mass and temperature in the thermal reservoir (Test Case 1)**

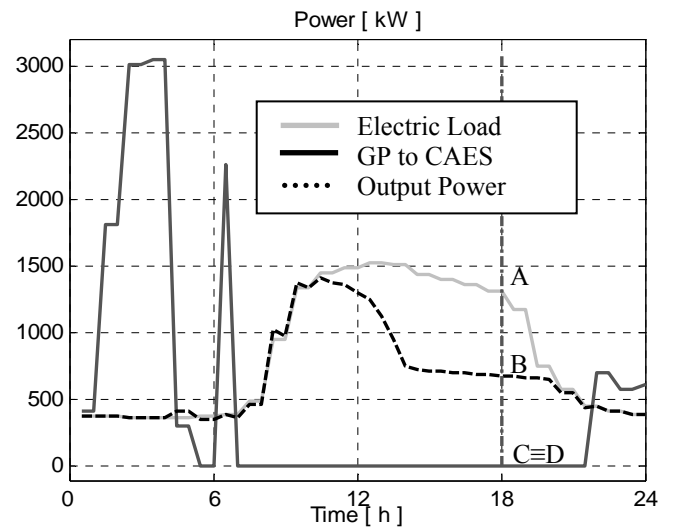


**Fig. 17 – Time history of electrical load, grid power and output power (Test Case 3A)**

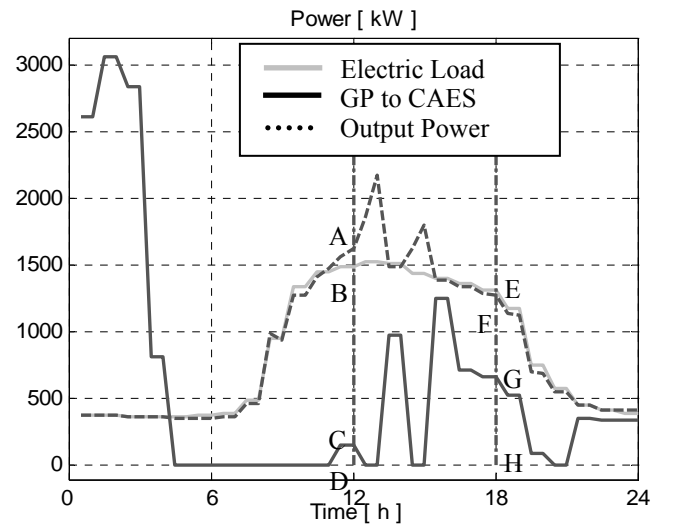


**Fig. 18 - Time history of electrical load, grid power and output power (Test Case 3B)**

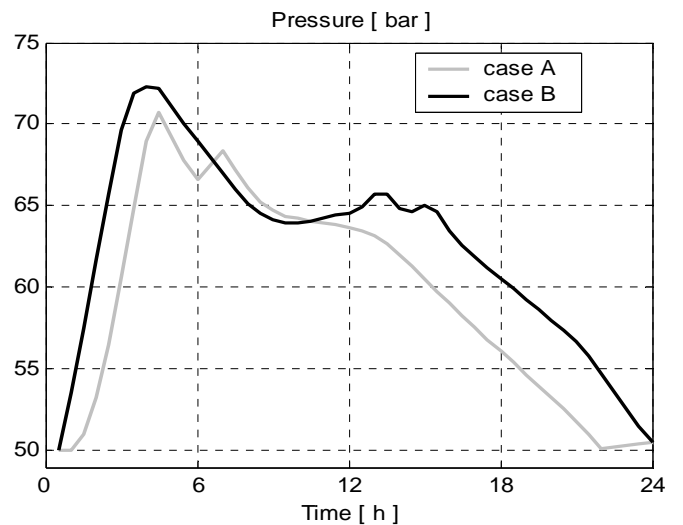


**Fig. 19 – Time history of pressure in the air reservoir (Test Cases 3A and 3B)**

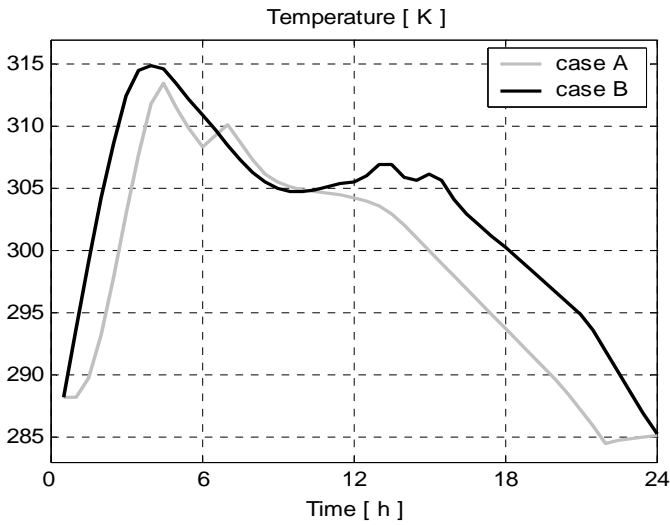


**Fig. 20 – Time history of temperature in the air reservoir (Test Cases 3A and 3B)**

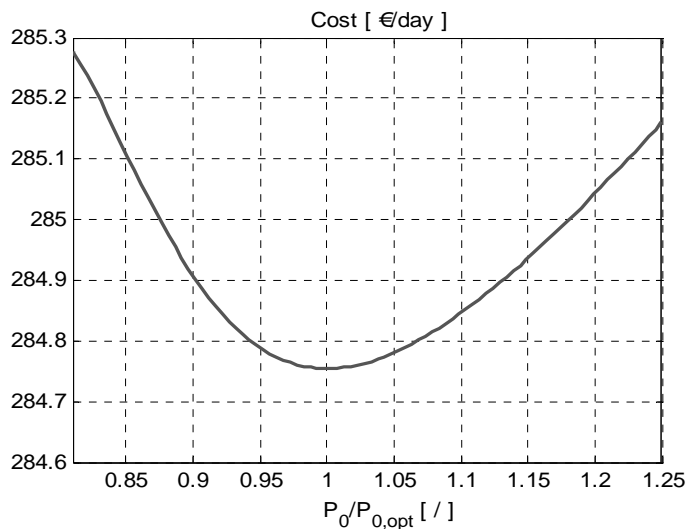


**Fig. 21 – Sensitivity Analysis: compressor design power vs. daily cost (test case 1)**

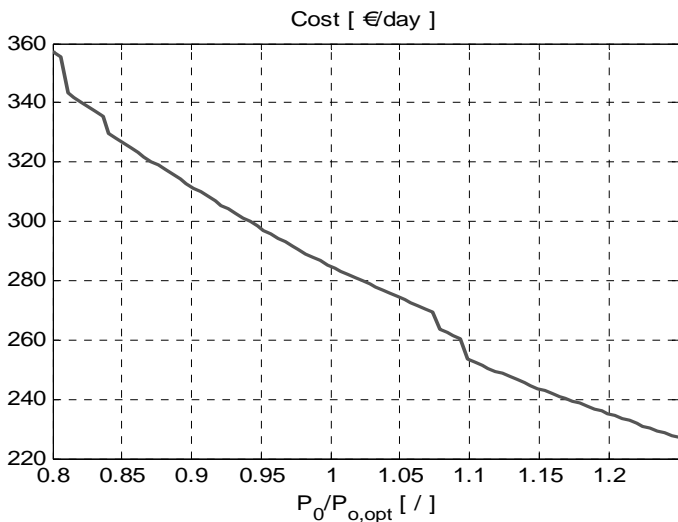


**Fig. 22 - Sensitivity Analysis: turbine design power vs. daily cost (test case 1)**

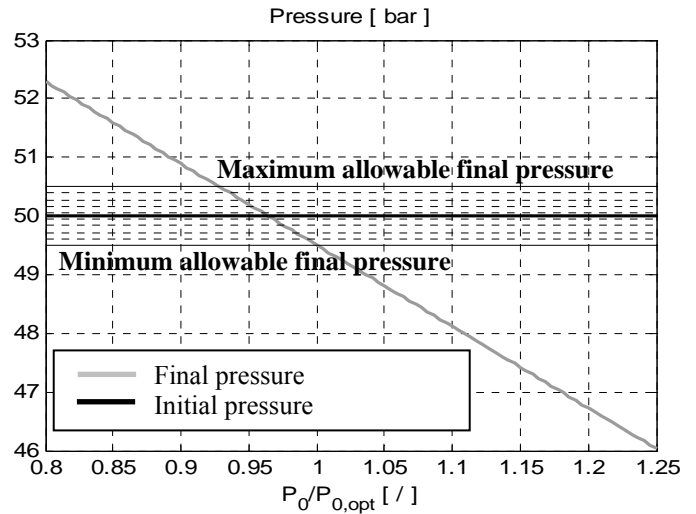


**Fig. 23 – Sensitivity Analysis: initial and final pressure in the air reservoir vs. design power of the turbine**

### MODEL COMPUTATIONAL REQUIREMENTS

AMD Athlon™ XP 2600, 1.95 GHz, 512 MB RAM

Cases	Optimization	Simulation
Case 1	28 min	0.095 s
Case 2	0.015 s	
Case 3 - A	17 min	0.1 s
Case 3 - B	49 min	0.1 s
Case 4	0.015 s	

**Tab. IV – Computational Requirements**

### CONCLUSIONS AND FUTURE DEVELOPMENTS

The integration of a wind turbine with CAES and grid has been analyzed on a daily cycle, also comparing various alternative scenario's. The proposed optimization approach allows determining both design variables, as turbine and compressor rated power, and optimal management strategies, satisfying daily cycle periodicity constraints.

Although further reductions could be still achieved by proper algorithm optimization, the computational time is rather limited and still compatible with real-time application. To this purpose the model has to be integrated with proper provisional methods of both power demand and wind speed.

The results show that the integration of CAES with wind turbine and grid allows reducing daily operational costs and CO<sub>2</sub> emissions by a factor of 2 with respect to conventional use of wind turbine and grid, while the integration of CAES with grid allows saving from 20 to 25 % of the daily operational costs, but with negligible benefits on emissions. The adoption of CAES and wind turbine allows cutting about 90% of daily operational costs and CO<sub>2</sub> emissions with respect to the sole recourse to grid: it is also evident that a proper comparison between different plant options should also account for the investment costs, not yet included in the model, and Life Cycle Assessment.

The presented results also evidence that the design of all plant components (wind turbine, compressor, reservoir and turbine) are strictly connected each other and also depending on management strategy and time distribution of incoming energy and electric load. Further studies are needed to analyze the relationships between these variables, in order to determine both the optimal plant configurations and the corresponding management strategies according to plant location and user demand.

Future developments will consist in:

- Enhancement of the economic model, including the estimation of investment costs.
- Integration of solar thermal panels in the plant layout.
- Development of provisional methods to estimate both incoming energy (wind/solar) and power demand, and their integration in the optimization model for real-time application.

## REFERENCES

- [1] El Wakil M.M., 1984, *Power Plant Technology*, McGraw Hill.
- [2] Ackermann T., Söder L., 2002, "An Overview of Wind Energy-Status 2002", *Renewable and Sustainable Energy Reviews*, **6** (2002) 67–128.
- [3] Celik A.N., 2002, "Optimisation and Techno-Economic Analysis of Autonomous Photovoltaic–Wind Hybrid Energy Systems in Comparison to Single Photovoltaic and Wind Systems", *Energy Conversion and Management*, **43** (2002) 2453–2468.
- [4] Habib M.A., Said S.A.M., El-Hadidy M.A., Al-Zaharna I., 1999, "Optimization Procedure of a Hybrid Photovoltaic Wind Energy System", *Energy*, **24** (1999) 919–929.
- [5] Beyer H.G., Degner T., 1997, "Assessing the Maximum Fuel Savings Obtainable in Simple Wind-Diesel Systems", *Solar Energy*, **61**, pp.5-10, (1997).
- [6] Elhadidy M.A., Shaahid S.M., 1999, "Optimal Sizing of Battery Storage for Hybrid (Wind + Diesel) Power Systems", *Renewable Energy* **18** (1999) 77-86.
- [7] Elhadidy M.A., Performance Evaluation of Hybrid (Wind/Solar/Diesel) Power Systems, *Renewable Energy*, **26** (2002) 401–413.
- [8] Elhadidy M.A., Shaahid S.M., 2000, "Parametric Study of Hybrid (Wind + Solar + Diesel) Power Generating Systems", *Renewable Energy*, **21** (2000) 129-139.
- [9] McGowan J.G., Manwell J.F., 1999, "Hybrid PV/Wind/Diesel Experiences", *Renewable Energy*, **16** (1999), 928-933.
- [10] Korpaasa M., Holena A.T., Hildrumb R., 2003, "Operation and Sizing of Energy Storage for Wind Power Plants in a Market System", *Electrical Power and Energy Systems*, **25** (2003) 599–606.
- [11] Najjar Y.S.H., Zaamout M.S., 1998, "Performance Analysis of Compressed Air Energy Storage (CAES) Plant for Dry Regions", *Energy Conversion Management*, **39**, No. 15, pp. 1503-1511, (1998)
- [12] Shnaid I., Weiner D., Brokman S., 1997, "Compressed Air Energy Storage Method and System", *Renewable Energy*, **11**, Issue: 2, June, 1997, pp. 282.
- [13] Daly J., Loughlin R. M., De Corso M., Moen D., Davis L., 2001, "CAES. Reduced to Practice", *Proceedings of ASME Turbo Expo 2001*, June 4-7, 2001, New Orleans, Louisiana.
- [14] Arnulfi G. L., Marini M., 2003, "Analysis of Transient Performance of a Compressed Air Energy Storage Plant", *Proc. of ASME Turbo Expo 2003 Power for Land, Sea and Air*, June 16-19, 2003, Atlanta, Georgia, USA.
- [15] Holden P., Moen D., De Corso M., Howard J., 2000, "Alabama Electric Cooperative Compressed Air Energy Storage (CAES) Plant Improvements", *Proc. Of ASME Turbo Expo 2000*, May 8-11, 2000, Munich Germany, 2000.
- [16] Nakhmkin M., Van Der Linden S., 2000, "Integration of a Gas Turbine (GT) with a Compressed Air Storage (CAES) Plant Provides the Best Alternative for Mid-Range and Daily Cyclic Generation Needs", *Proc. Of ASME Turbo Expo 2000*, May 8-11, 2000, Munich Germany, 2000.
- [17] Nakhmkin M., Wolk R. H., Van Der Linden S., Patel M., 2004, "New Compressed Air Energy Storage Concept Improves the Profitability of Existing Simple Cycle, Combined Cycle, Wind Energy, and Landfill Gas Power Plants", *Proc. of ASME Turbo Expo 2004 Power for Land, Sea, and Air*, June 14-17, 2004, Vienna, Austria.
- [18] Takahashi K., Yasuda T., Endoh M., Kurosaki M., 2002, "Application of Dynamic Simulation to CAES G/T Control System Development", *Proc. of ASME Turbo Expo 2002*, June 3-6, 2002, Amsterdam, The Netherlands.
- [19] Greenblatt J. B., Succar S., Denkenberger D. C., Williams R. H., 2004, "Toward Optimization of a Wind/ Compressed Air Energy Storage (CAES) Power System", *Proc. of ASME Power 04 Conference*, Baltimore, MD, 30 March – 1 April 2004.
- [20] Muljadi E., Pierce K., Migliore P., 2000, "Soft-Stall Control for Variable-Speed Stall-Regulated Wind Turbines", *Journal of Wind Engineering and Industrial Aerodynamics*, **85** (2000) 277 - 291.
- [21] Porkhial S., Khastoo B., Modarres Razavi M.R., 2002, "Transient Characteristic of Reciprocating Compressors in Household Refrigerators", *Applied Thermal Engineering*, **22**, (2002) 1391 – 1402.
- [22] Zhang N., Ruixian Cai, 2002, "Analytical Solutions and Typical Characteristics of Part-Load Performances of Single Shaft Gas Turbine and its Cogeneration", *Energy Conversion and Management*, **43**, Issue: 9-12, June - August, 2002, pp. 1323-1337.
- [23] Arsie I., Marano V., Rizzo G., 2004, "A Model for Thermo-Economic Analysis and Optimization of Steam Power Plants for Power and Cogeneration", *Proc. of ASME Power 04 Conference*, Baltimore, MD, March 30-April 1, 2004.
- [24] Gambini M., Vellini M., 2000, "CO2 Emission Abatement from Fossil Fuel Power Plants by Exhaust Gas Treatment", *Proc. of 2000 Int. Joint Power Generation Conference*, Miami Beach, Florida, July 23-26, 2000.

- [25] Voorspools K.R., Brouwers E.A., D'Haeseleer W.D., 2000, "Energy Content and Indirect Greenhouse Gas Emissions Embedded in 'Emission-Free' Power Plants: Results for the Low Countries", *Applied Energy*, **67**, (2000) 307±330.
- [26] Gill, P.E., W. Murray, and M.H. Wright, 1981, *Practical Optimization*, Academic Press, London.
- [27] Zhao H., Holst J., Arvastson L., 1998, "Optimal Operation of Coproduction with Storage", *Energy* **23**, No. 10, pp. 859–866, 1998.
- [28] Nappi G., 2004, "Un Modello per il Progetto Ottimizzato di un Impianto di Potenza Ibrido CAES-Eolico", Thesis, DIMEC - University of Salerno (in Italian).

## **ACKNOWLEDGMENTS**

This research work has been financed by University of Salerno.